Biophysical Chemistry 198 (2015) 36–44

Contents lists available at ScienceDirect

Biophysical Chemistry

journal homepage: http://www.elsevier.com/locate/biophyschem

Cy3 and Cy5 dyes attached to oligonucleotide terminus stabilize DNA duplexes: Predictive thermodynamic model

Bernardo G. Moreira [1], Yong You, Richard Owczarzy *

Department of Molecular Genetics, Integrated DNA Technologies, 1710 Commercial Park, Coralville, IA 52241, USA

HIGHLIGHTS

- Cy3 and Cy5 dyes at termini stabilize DNA duplexes.
- Duplex stability is increased by 1.2 kcal/mol on average.
- The magnitude of stabilization depends on the base sequence.
- The dyes show larger thermodynamic effects than dangling nucleotides.

GRAPHICAL ABSTRACT

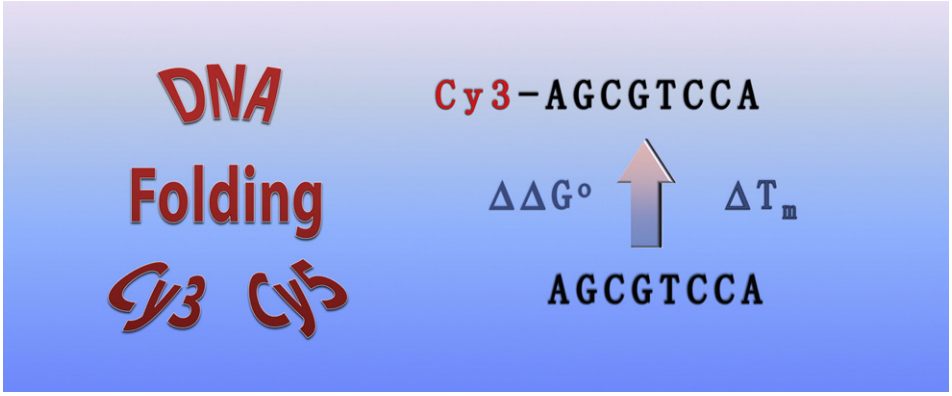

ARTICLE INFO

Article history:
Received 10 December 2014
Received in revised form 2 January 2015
Accepted 2 January 2015
Available online 8 January 2015

Keywords:
Cyanine
Fluorescence
Nucleic acid
Nearest neighbor
Melting temperature

ABSTRACT

Cyanine dyes are important chemical modifications of oligonucleotides exhibiting intensive and stable fluorescence at visible light wavelengths. When Cy3 or Cy5 dye is attached to 5′ end of a DNA duplex, the dye stacks on the terminal base pair and stabilizes the duplex. Using optical melting experiments, we have determined thermodynamic parameters that can predict the effects of the dyes on duplex stability quantitatively (ΔG°, T_m). Both Cy dyes enhance duplex formation by 1.2 kcal/mol on average, however, this Gibbs energy contribution is sequence-dependent. If the Cy5 is attached to a pyrimidine nucleotide of pyrimidine–purine base pair, the stabilization is larger compared to the attachment to a purine nucleotide. This is likely due to increased stacking interactions of the dye to the purine of the complementary strand. Dangling (unpaired) nucleotides at duplex terminus are also known to enhance duplex stability. Stabilization originated from the Cy dyes is significantly larger than the stabilization due to the presence of dangling nucleotides. If both the dangling base and Cy3 are present, their thermodynamic contributions are approximately additive. New thermodynamic parameters improve predictions of duplex folding, which will help design oligonucleotide sequences for biophysical, biological, engineering, and nanotechnology applications.

Abbreviations: C_t, total single strand concentration; Cy, Cy3 or Cy5 dye; ΔG°_{37}, transition Gibbs free energy at 37 °C; ΔH°, transition enthalpy; ΔS°, transition entropy; T_m, melting temperature, SVD, singular value decomposition

* Corresponding author. Tel.: +1 319 626 8459.
E-mail address: science@owczarzy.net (R. Owczarzy).
URL: http://biophysics.idtdna.com (R. Owczarzy).
[1] Present address: Hawkeye Community College, 1501 E Orange Rd, Waterloo, IA 50701, USA.

http://dx.doi.org/10.1016/j.bpc.2015.01.001

1 . Introduction

Many biophysical and biological studies use oligonucleotides that contain additional chemical moieties attached to either 5′ or 3′ terminus. These moieties provide DNA oligomers with useful and unique properties. Cy dyes are one important class of such modifications. The dyes have sharp absorption bands, high extinction coefficients, excellent resistance to photobleaching and make DNA oligomers highly fluorescent, so that even single molecules can be observed [1,2]. Their chemical structure is built from two indole rings that are connected by a polymethine chain (Fig. 1). Cy3 dye (1,1′-bis(3-hydroxypropyl)-3,3,3′,3′-tetramethylindo carbocyanine) contains a connecting chain of *three* methine groups. The chain consists of *five* methine groups in Cy5 dye (1,1′-bis(3-hydroxypropyl)-3,3,3′,3′-tetramethylindodicarbocyanine).

In the case of oligonucleotides, the dyes are often linked to the ribose at 5′ terminus. In our experiments, the covalent linker consisted of 5′ phosphate group and the propyl chain that was connected to indole ring. Cyanine-modified oligonucleotides have been used in numerous studies of composition, structure and dynamics of nucleic acids including genotyping [3–5], real-time PCR [4,6,7], gene expression, microarray experiments [8,9], molecular beacons [10], *in situ* hybridizations [11], single molecule dynamics investigations [1,12,13], nanoparticles [8,14], optical switches for data storage [15], enzyme kinetics [16] and protein–nucleic acid interactions [17]. Typically, annealing of the probe to its target alters the fluorescence properties of the cyanine-labeled oligonucleotide. This could be accomplished by various schemes of dye quenching [4,18]. Another set of applications relies on Förster resonance energy transfer (FRET) between pair of dyes, allowing measurements of distances on nanometer scale [19]. For example, pairing of Cy3 with Cy5 is favored in single molecule studies [20]. Many aspects of Cy3 and Cy5 *fluorescent* properties have been investigated [2,21–23]. Levitus and Ranjit recently reviewed cyanine dye photophysics [24]. Our interest is focused on the energetics of molecular interactions.

Design of experiments and applications relies on predictions of melting temperatures (T_m) and Gibbs energies (ΔG°) of hybridization. The nearest-neighbor thermodynamic model has been very successful in predicting energetics and extent of hybridization for native DNA [25,26] and RNA duplexes [27,28]. Additional chemical groups can significantly affect duplex stability and melting temperature. We have observed that many dyes and quenchers attached to duplex terminus increase T_m values [29]. Cy dyes appear to stabilize DNA duplexes most from a group of seven common fluorescent dyes [29].

It has not been possible to model the dye effects accurately because sequence specificity of the stabilization has not been studied. We therefore measured and determined sequence-dependent thermodynamic parameters for Cy3 and Cy5 dyes attached to a terminal nucleotide. New parameters are compatible with the published nearest-neighbor model of DNA duplexes [26] and improve accuracy of T_m and ΔG° predictions. The results are important not only for oligonucleotide design, but also for interpretation of structure, dynamics and photophysics of Cy-modified nucleic acid molecules.

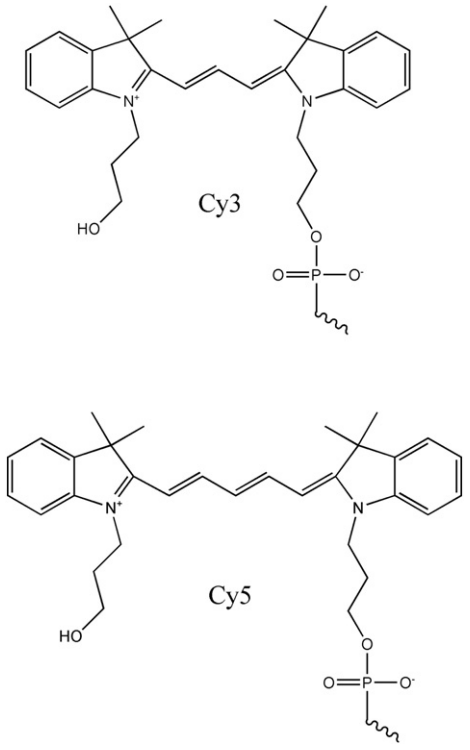

Fig. 1. Chemical structures of cyanine dyes and their attachment to 5′ terminus of oligonucleotides *via* phosphate group.

2. Materials and methods

2.1. Oligonucleotide synthesis

Oligodeoxynucleotides were chemically synthesized using phosphoramidites at Integrated DNA Technologies (Coralville, IA). DNA samples were purified with Transgenomic Wave HPLC system and/or 8 M urea denaturing polyacrylamide gel electrophoresis [29]. Attachment of dyes and purity of oligonucleotides were verified by electrospray-ionization liquid chromatography mass spectroscopy (ESI-LCMS). These tests were done on an Oligo HTCS system (Novatia, Princeton, NJ). Samples were discarded if the experimental molecular mass of oligonucleotide deviated more than 2 g/mol from the expected molecular mass. Oligonucleotide lots were also analyzed by capillary electrophoresis that was run using a Beckman PACE 5000 or Beckman MDQ systems [30]. Oligonucleotides that were less than 90% pure were purified again until they reached this level of purity. These assays confirmed quality and identity of oligonucleotides.

2.2 . UV melting experiments

We followed our published experimental protocol [30]. Oligonucleotides were rehydrated in 50 mM Na^+ buffer (50 mM NaCl, 10 mM phosphate, 1.0 mM Na_2EDTA, pH = 7.0) and their concentrations were determined from absorbance measurements at 260 nm using two different dilutions. Absorbance of self-complementary sequences was read at 85 °C to denature all base pairs. Extinction coefficients of oligomers were predicted from the nearest-neighbor model [31]. Extinction coefficients of Cy3 and Cy5 at 260 nm were added — they were assumed to be 4900 and 10,000 $L \cdot mol^{-1} \cdot cm^{-1}$, respectively [29]. Concentrated stocks of duplexes were prepared by mixing of strands in 1:1 molar ratio, heating the sample to 95 °C, and slowly cooling to ambient temperature.

Melting buffer consisted of 1 M NaCl, 10 mM sodium phosphate, 1 mM Na_2EDTA, adjusted with NaOH to pH 7.0. DNA stock samples were dialyzed against the melting buffer in 28-Well Microdialysis System (Gibco-BRL, Gaithersburg, MD) for at least 24 h. Samples for melting experiments were made by direct dilutions from the stock solution. UV melting profiles were measured using a Beckman DU 650 spectrophotometer with Micro T_m Analysis accessory. Absorbance values at 268 nm were recorded every 0.1 °C. Sample heating rate was 25 °C/h. Temperatures were obtained from an internal probe located inside of the Peltier holder and corrected based on our previous calibration measurements [30]. Custom-made 1 mm and 10 mm pathlength cuvettes (Helma GmbH, Müllheim, Germany) allowed us to measure total single strand concentrations (C_t) ranging from 1 to 175 μM. Absorbance of the upper baseline extrapolated to 25 °C was used to verify proper dilutions of samples and to estimate experimental C_t concentrations.

2.3 . Determination of thermodynamic parameters

We employed the published procedure [30] to transform absorbance melting data to the fraction of dissociated base pairs (θ). T_m was determined as the temperature [32] where $\theta = 0.5$. Each sample was measured in two different positions of the 6-cuvette Peltier holder to reduce experimental errors. Average standard deviation of T_m measurements was 0.5 °C for the primary data set and 0.3 °C for the validation data set.

Thermodynamic parameters were obtained from melting profiles by using two different approaches. The first method was based on the integrated form of van't Hoff equation [32,33],

$$-\ln K_{eq} = \frac{\Delta H^\circ}{R}\frac{1}{T} - \frac{\Delta S^\circ}{R} \quad (1)$$

The equilibrium constant of hybridization reaction (K_{eq}) was estimated at each temperature T,

$$K_{eq} = \frac{m(1-\theta)}{\theta^2 C_t} \quad (2)$$

where m is the constant equal to ½ for a duplex formed from a single self-complementary strand and 2 for a duplex annealed from two different strands [32,34].

As expected from Eq. (1), the plots of ln K *versus* $1/T$ showed linear relationships in the transition region where θ ranges from 0.15 to 0.85. The plots were fitted to straight lines whose slopes and intercepts were used to calculate ΔH° and ΔS° values [33,35]. From four to eight heating and cooling melting profiles were averaged for each DNA sample to determine the transition enthalpy, entropy and Gibbs energy. The thermodynamic values were further averaged over various DNA concentrations. If absorbance values were below 0.1 or above 1.0, ln K_{eq} fits had large errors due to spectrophotometer limitations and experimental noise. In this case, the thermodynamic data were excluded from the ΔH°, ΔS°, ΔG°_{37} averages. However, experimental melting temperatures were robust and exhibited similar errors regardless of absorbance value. T_m values from all experiments were therefore included in the following analysis.

In the second method, melting temperatures were determined at twelve different DNA concentrations for each duplex sequence (see concentrations in Table S1 of the Supplementary data). Reciprocal melting temperatures were plotted as a function of ln C_t. Thermodynamic values were determined from slopes and intercepts of linear fits [25,33–36] according to the relationship,

$$\frac{1}{T_m} = \frac{\Delta S^\circ}{\Delta H^\circ} + \frac{R}{\Delta H^\circ}\ln\frac{C_t}{i} \quad (3)$$

where R is the ideal gas constant. The constant i reflects differences in molecularity of annealing reaction — it equals to 1 for self-complementary strands and 4 for duplexes annealed from two different strands. If a data point deviated from the fitted straight line more than three times of its estimated error, it was deemed to be the outlier. The outlier was discarded and melting experiments were often repeated. Less than 5% of all melting data points appeared to be such outliers. Since absorbance values would range from 0.1 to 12.4 in 10 mm pathlength cuvette, the samples of absorbance above 1.4 were measured in 1 mm cuvette. To explore the largest possible range of absorbance values, the oligonucleotide concentrations decreased somewhat with the duplex length (Supplementary Table S1). Samples having absorbance value of 1.42 were measured in both 10 mm and 1 mm cuvettes to compare and eliminate systematic errors due to cuvette sizes. The oligonucleotide concentrations were designed to be uniformly distributed on the logarithmic scale, *i.e.*, differences between consecutive ln C_t data points were nearly identical.

Both analysis methods assumed that the melting process proceeds in the two-state manner and the change of heat capacity between the single-strands and the duplex is negligible. If ΔH° values or ΔS° values differed by more than 15% between both methods, the two-state assumption was considered invalid and the thermodynamic data were not used to determine thermodynamic parameters [25,33,35].

Gibbs energy contributions of dyes have been calculated as a difference between modified and the corresponding core duplexes. For example, the contribution for Cy3–AG sequence context was obtained from the following difference,

$$\Delta\Delta G^\circ(\text{Cy3—AG}) = \Delta G^\circ(\text{Cy3—AGCGTCCA/TCGCAGGT}) - \Delta G^\circ(\text{AGCGTCCA/TCGCAGGT}) \quad (4)$$

Enthalpic and entropic contributions have been estimated using analogous differences.

Thermodynamic parameters were extracted from thermodynamic values using previously published analysis based on singular value decomposition [37]. The fitted parameters minimized χ^2 for a set of oligonucleotide measurements,

$$X^2 = \left|\left(\mathbf{M}\times\mathbf{P}-\mathbf{E}^x\right)\times\sigma_E^{-1}\right|^2 \quad (5)$$

where $\mathbf{P}$ is the vector of unknown parameters, $\mathbf{E}^x$ is the column vector of experimentally measured thermodynamic contributions attributed to cyanine dye ($\Delta\Delta G^\circ_{37}$, $\Delta\Delta H$, or $\Delta\Delta S^\circ$), and σ_E is the diagonal matrix of experimental errors. The design matrix $\mathbf{M}$ contains the number of occurrences of each parameter in each duplex. The definition of parameters and their occurrences depends on the model. We have investigated models based on a single parameter, nearest neighbors, next nearest neighbors, neighbor purines/pyrimidines, *etc.*

The fits were not weighted based on experimental errors because this could introduce artifacts. We did not expect accuracy of thermodynamic values to vary substantially from one duplex sequence to another. Values of σ_E were therefore set to average errors that were estimated by error propagation (2.1 kcal·mol^{-1} for $\Delta\Delta H^\circ$, 6.4 kcal·mol^{-1}·K^{-1} for $\Delta\Delta S^\circ$, and 0.2 kcal·mol^{-1} for $\Delta\Delta G^\circ_{37}$). The goodness-of-fit and accuracy of prediction was judged by calculating χ^2 and root mean square deviation (rmsd) over a data set of n measurements,

$$\text{rmsd} = \sqrt[2]{\frac{\sum_{i=1}^{n}\left(E^p - E^x\right)^2}{n}} \quad (6)$$

where $E^p - E^x$ is the difference between predicted and experimentally measured thermodynamic values.

3. Results

3.1 . Ultraviolet melting experiments

We have studied stability of DNA duplex oligomers where Cy dyes were attached to the 5′ terminus. Several chemical variants have been defined as Cy3 and Cy5 in the published literature. Fig. 1 shows the chemical structures of our dyes and their tethers. Our molecules do not contain a sulfonate group in position 5 of indole rings, which is sometimes introduced to increase water solubility. These Cy modifications are commercially available from many sources (Integrated DNA Technologies, Coralville, IA). Fig. 2A presents an example of the set of experimental melting profiles that were done for each duplex. Both dye-modified and native duplexes showed profiles characteristic of a single transition, which had sigmoidal shape. Heating and cooling melting profiles were superimposable within experimental errors indicating that the melting transitions for all samples were reversible and close to equilibrium.

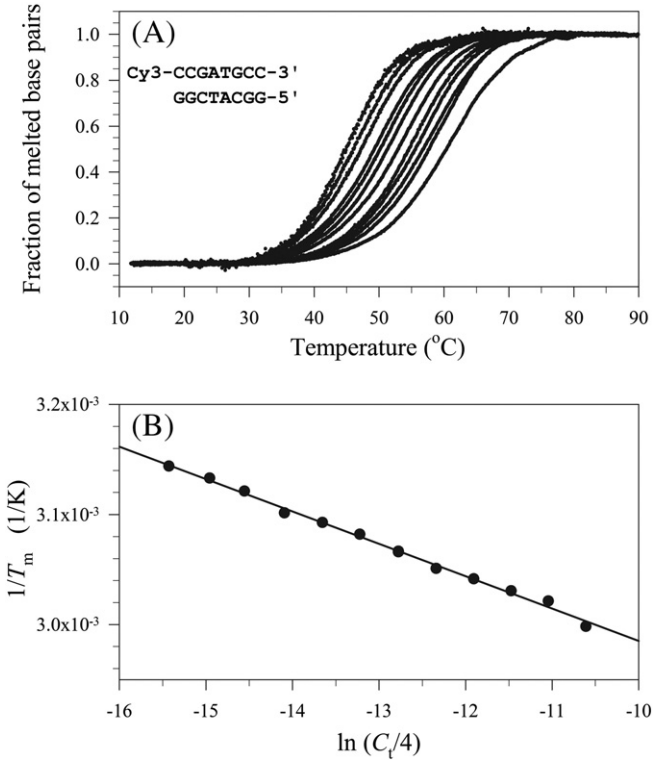

Fig. 2. Example of thermodynamic analysis for D19 duplex. (A) Melting profiles averaged at each oligonucleotide concentration. (B) Fit of melting temperatures to determine ΔH°, ΔS°, and ΔG°_{37} values.

Sequences and thermodynamic values of the primary data set are reported in Table 1. The set contained 35 modified oligomer duplexes. For comparison, 10 unmodified core duplexes of the same sequences were also measured. This data allowed us to determine Gibbs energy contributions attributed to stabilizing effects of Cy dyes. The sequences were designed to exhibit melting temperatures in the range from 35 to 75 °C, so that linear baselines before and after melting transition were measured. The well-defined baselines decreased uncertainties of thermodynamic analysis. The sequences were selected to be short, from 8 to 12 base pairs, resulting in significant Gibbs energy contributions of dyes to the total ΔG° of duplex hybridization. In addition, short DNA duplexes are likely to melt in two-state manner, simplifying thermodynamic analysis. Sequences were also chosen to minimize formation of alternative secondary structures such as hairpins and partially complementary duplexes.

Thermodynamic values of duplex melting reaction were determined from fits to individual melting profiles and from plots of $1/T_m$ vs ln C_t. The plots are depicted in Fig. 2B and 1S in the Supplementary data. The relationships are linear as expected for two-state melting process. The ΔH° values differed less than 12% between two analytical methods and average difference was 4.6%. For ΔS°, the largest difference was 14% and the average deviation was 5.2%. The ΔG°_{37} differences were less than 0.8 kcal/mol between two methods and the average difference was 0.2 kcal/mol. These results are consistent with two-state melting behavior [35,38]. The assumption of single cooperative transition appears to be reasonable for all duplexes.

3.2 . Thermodynamic models of Cy3 and Cy5 terminal modifications

The primary set (Table 1) includes variety of sequences because we attempted to explore many factors that could influence thermodynamic effects of dyes. Four sequences were self-complementary. The other duplexes were annealed from two different sequences. At the site of dye attachment, all sixteen possible nearest neighbors (AA, AC, AG, AT, CA, *etc.*) were present in the data set. In some cases, two dyes were attached, one to each terminus of a duplex, essentially doubling the thermodynamic effects.

Results in Table 1 demonstrate that Cy dyes are always stabilizing and increases melting temperature regardless of neighboring oligonucleotide sequence. The impact of modifications on melting temperatures (ΔT_m) is expected to be more significant for short oligomers than for long oligomers. This is observed experimentally. Average ΔT_m per Cy3 modification decreased from 6.0 °C for 8-mers to 3.9 °C for 12-mers. A similar decrease has been observed for Cy5 oligonucleotides, from 6.0 to 3.8 °C. However, true thermodynamic values, *e.g.*, Gibbs energy changes per modification, are independent of duplex length.

It was previously shown that Texas Red and Iowa Black RQ quencher do not affect thermodynamic stability beyond two base pairs from duplex terminus [39]. We have anticipated that the Cy dyes also interact mostly with a few of the closest base pairs and long interactions have negligible impacts on duplex energetics. This notion was examined by comparison of singly and doubly modified duplexes. If a duplex contains a dye at each terminus and the distance between the dyes is large enough to suppress significant interactions, the stabilizing effects are expected to be additive. Table 2 shows that stabilizing Gibbs energies originating from each terminus are indeed additive within experimental errors. No significant energetic interactions are therefore occurring between two cyanine dyes attached at the opposite ends of a duplex. This result suggests that Cy3 thermodynamic effects are localized to oligonucleotide 5′ terminus and do not extend more than 4 base pairs (half of the measured duplexes).

We have tested several models of various complexities in the search for the most suitable thermodynamic model. The simplest model, the one-parameter model (1P) assumes that the thermodynamic contribution of a dye is independent of oligonucleotide sequence and could be described by a single parameter for each dye. The fitted parameters of the model are presented at the top of Supplementary Table S2. Average stabilizing Gibbs energy of Cy3 modification is −1.2 kcal/mol. The same average change of Gibbs energy is seen for Cy5 dyes within the experimental error. We have next analyzed sequence dependence of thermodynamic effects.

Fig. 3 shows Gibbs energy contributions attributed to the dye as a function of the nearest nucleotide. The solid line connects average values and demonstrates the trend. Significant sequence dependence is seen for both Cy3- and Cy5-modified oligonucleotides. If Cy dye is attached to a pyridine nucleotide, it tends to stabilize the duplex more (−1.4 kcal/mol) than the Cy dye attached to a purine nucleotide (−1.0 kcal/mol). The only exception is Cy3-T-sequence context, which is less stabilizing than expected. The 1P model does not account for these sequence-specific effects. The better model would consider the type of the nearest base pair and the nucleotide conjugated to the dye. Parameters of such model, the nearest-neighbor model (NN), are reported in the bottom of Table S2. They were determined from the fit to the primary data set.

Close examination of the melting data indicates that interactions between the dyes and the nearest base pair are not sufficient to model variations in the thermodynamic contributions shown in Fig. 3. The substantial deviations of $\Delta\Delta G^\circ_{37}$ values are seen within each group of the same x-axis value. For example, $\Delta\Delta G^\circ_{37}$ of Cy5–AC/TG is −1.2 kcal/mol while $\Delta\Delta G^\circ_{37}$ of Cy5–AA/TT is −0.5 kcal/mol. The difference between these values, 0.7 kcal/mol, is significantly higher than the estimated experimental errors (±0.2 kcal/mol). The substantial Gibbs energy differences are also seen between Cy5–TA/AT and Cy5–TC/AG as well as between Cy3–TA/AT and Cy3–TG/AC (0.4 kcal/mol). These observations suggest that the next-nearest-neighbor model (NNN) could improve accuracy of the predictions. The model contains sixteen parameters to account for each possible combination of the dye and two neighboring base pairs. The fitted parameters are presented in Table 3 for both Cy3 and Cy5 modifications. Calculation of duplex stability using these parameters is illustrated in the Supplementary data.

Table 1
Thermodynamic values of single strand-duplex annealing reactions in 1 M Na^+ buffer.

ID	Duplex DNA sequences (5′–3′/3′–5′)[a]	$\Delta H°$ (kcal·mol^{-1})[b]	$\Delta S°$ (cal·mol^{-1}·K^{-1})[b]	$\Delta G°_{37}$ (kcal·mol^{-1})[b]	T_m (°C)[c]	ΔT_m (°C)[d]
	Core duplexes					
D1	ACGATCGT/TGCTAGCA	−58.5	−161.8	−8.3	38.4	
D2	CTGATCAG/GACTAGTC	−62.1	−176.6	−7.3	33.2	
D3	GATGCATC/CTACGTAG	−60.6	−171.4	−7.4	33.7	
D4	TCACGTGA/AGTGCACT	−58.8	−165.1	−7.6	34.7	
D5	AGCGTCCA/TCGCAGGT	−58.5	−157.3	−9.7	41.2	
D6	GGCATCGG/CCGTAGCC	−65.5	−179.3	−9.9	41.5	
D7	ATCGTTGCTA/TAGCAACGAT	−68.0	−185.6	−10.4	44.0	
D8	CAGCAGGCAC/GTCGTCCGTG	−73.1	−196.6	−12.1	51.2	
D9	GCGAGGAGGCTT/CGCTCCTCCGAA	−91.3	−244.9	−15.3	60.3	
D10	TTCAAGTATTCG/AAGTTCATAAGC	−82.3	−230.5	−10.8	44.3	
	Cy3-modified duplexes					
D11	Cy3–ACGATCGT/TGCTAGCA–Cy3	−66.1	−178.2	−10.9	50.7	12.3
D12	Cy3–CTGATCAG/GACTAGTC–Cy3	−66.1	−180.9	−10.0	46.1	12.9
D13	Cy3–GATGCATC/CTACGTAG–Cy3	−66.6	−182.6	−9.9	45.9	12.2
D14	Cy3–TCACGTGA/AGTGCACT–Cy3	−61.0	−164.9	−9.9	46.4	11.7
D15	Cy3–AGCGTCCA/TCGCAGGT	−63.2	−168.8	−10.8	46.6	5.4
D16	Cy3–AGCGTCCA/TCGCAGGT–Cy3	−65.3	−172.1	−11.9	51.9	10.7
D17	AGCGTCCA/TCGCAGGT–Cy3	−64.9	−173.4	−11.1	47.7	6.5
D18	Cy3–GGCATCGG/CCGTAGCC	−71.9	−195.3	−11.3	47.5	6.0
D19	GGCATCGG/CCGTAGCC–Cy3	−67.7	−182.4	−11.2	47.6	6.1
D20	Cy3–ATCGTTGCTA/TAGCAACGAT	−73.8	−200.3	−11.7	48.9	4.9
D21	ATCGTTGCTA/TAGCAACGAT–Cy3	−70.1	−189.5	−11.3	47.9	3.9
D22	Cy3–CAGCAGGCAC/GTCGTCCGTG	−78.1	−208.3	−13.5	56.3	5.1
D23	CAGCAGGCAC/GTCGTCCGTG–Cy3	−76.1	−202.7	−13.2	55.5	4.3
D24	Cy3–GCGAGGAGGCTT/CGCTCCTCCGAA	−92.9	−246.5	−16.4	64.1	3.8
D25	Cy3–GCGAGGAGGCTT/CGCTCCTCCGAA–Cy3	−97.5	−257.9	−17.5	66.8	6.5
D26	GCGAGGAGGCTT/CGCTCCTCCGAA–Cy3	−93.8	−250.3	−16.2	62.9	2.6
D27	Cy3–TTCAAGTATTCG/AAGTTCATAAGC	−86.0	−238.9	−11.9	48.2	3.9
D28	Cy3–TTCAAGTATTCG/AAGTTCATAAGC–Cy3	−90.2	−247.5	−13.4	53.3	9.0
D29	TTCAAGTATTCG/AAGTTCATAAGC–Cy3	−86.6	−239.4	−12.4	49.8	5.5
	Cy5-modified duplexes					
D30	Cy5–ACGATCGT/TGCTAGCA–Cy5	−64.8	−174.3	−10.8	50.4	12.0
D31	Cy5–CTGATCAG/GACTAGTC–Cy5	−65.5	−178.5	−10.1	47.1	13.9
D32	Cy5–GATGCATC/CTACGTAG–Cy5	−63.7	−174.4	−9.6	44.6	10.9
D33	Cy5–TCACGTGA/AGTGCACT–Cy5	−66.0	−178.4	−10.7	49.8	15.1
D34	Cy5–AGCGTCCA/TCGCAGGT	−61.1	−162.4	−10.7	46.2	5.0
D35	AGCGTCCA/TCGCAGGT–Cy5	−62.0	−164.4	−11.0	47.7	6.5
D36	Cy5-GGCATCGG/CCGTAGCC	−66.7	−180.1	−10.8	46.0	4.5
D37	GGCATCGG/CCGTAGCC–Cy5	−65.2	−174.3	−11.1	47.7	6.2
D38	Cy5–ATCGTTGCTA/TAGCAACGAT	−71.0	−192.0	−11.5	48.4	4.4
D39	ATCGTTGCTA/TAGCAACGAT–Cy5	−71.5	−193.4	−11.5	48.7	4.7
D40	Cy5–CAGCAGGCAC/GTCGTCCGTG	−76.9	−204.3	−13.5	56.5	5.3
D41	CAGCAGGCAC/GTCGTCCGTG–Cy5	−75.6	−201.1	−13.2	55.7	4.5
D42	Cy5–GCGAGGAGGCTT/CGCTCCTCCGAA	−90.2	−239.2	−16.0	63.4	3.1
D43	GCGAGGAGGCTT/CGCTCCTCCGAA–Cy5	−90.7	−241.1	−15.9	62.7	2.4
D44	Cy5–TTCAAGTATTCG/AAGTTCATAAGC	−90.6	−252.4	−12.3	49.0	4.7
D45	TTCAAGTATTCG/AAGTTCATAAGC–Cy5	−86.6	−239.4	−12.3	49.6	5.3

[a] Before the slash, the sequence is shown in 5′ to 3′ direction. After the slash, the complementary strand sequence is in 3′ to 5′ orientation.
[b] Average values from melting curve fits and $1/T_m$ *versus* ln C_t plots.
[c] Melting temperatures are reported at C_t of 2 μM.
[d] Difference of melting temperatures between modified and core duplexes.

3.3 . *Performance of thermodynamic models*

We have examined accuracy of predictions made by new models and parameters. Performance was tested by calculating χ^2 and root mean square deviation values. Measurements of melting temperatures and Gibbs energy changes exhibit the lowest relative errors due to correlation and compensation of $\Delta H°$ and $\Delta S°$ errors [27]. We have therefore focused on predictions of experimental $\Delta\Delta G°_{37}$ and ΔT_m values

Table 2
Additivity of stabilizing Gibbs energies (kcal.mol^{-1}) for DNA duplexes labeled with one or two Cy3 dyes.

ID	Duplex DNA sequences (5′–3′/3′–5′)	ΔΔG°37 (Cy3 on left strand)[a]	$\Delta\Delta G°_{37}$ (Cy3 on right strand)[a]	$\Delta\Delta G°_{37}$ (sum)[b]	$\Delta\Delta G°_{37}$ (Cy3 on both strands)[a]
D16	Cy3-AGCGTCCA/TCGCAGGT-Cy3	−1.1	−1.4	−2.5	−2.2
D25	Cy3-GCGAGGAGGCTT/CGCTCCTCCGAA-Cy3	−1.1	−0.8	−1.9	−2.2
D28	Cy3-TTCAAGTATTCG/AAGTTCATAAGC-Cy3	−1.1	−1.5	−2.6	−2.6

[a] All thermodynamic values were experimentally measured. Differences of transition Gibbs energies between labeled and unlabeled duplexes are shown, $\Delta\Delta G° = \Delta G°$(labeled) − $\Delta G°$(native duplex).
[b] Sum of stabilizing Gibbs energies for two duplexes each labeled with a single Cy3 modification, $\Delta\Delta G°$(sum) = $\Delta\Delta G°$(left strand label) + $\Delta\Delta G°$(right strand label).

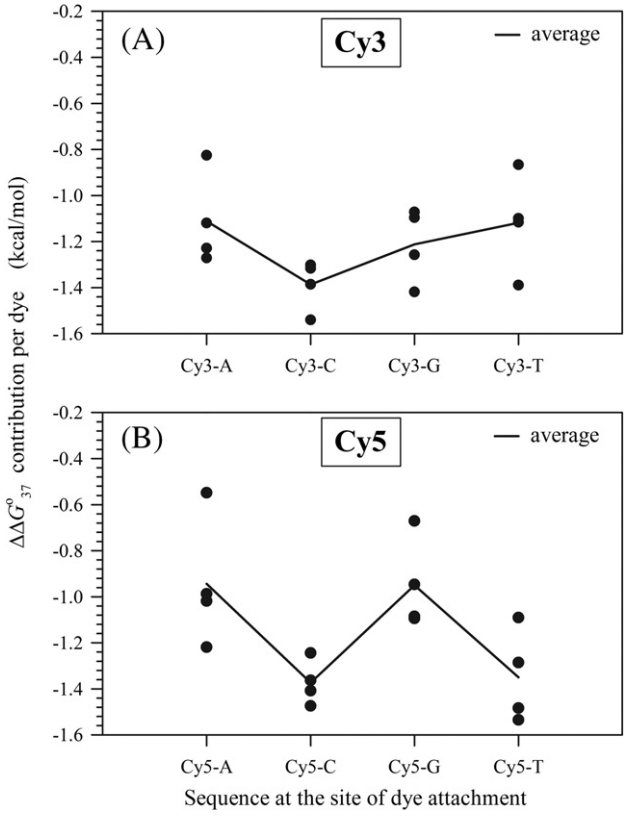

Fig. 3. Effects of the nearest base pair on the Gibbs energy contribution of cyanine dyes to duplex stability. Solid line connects average values to illustrate the trend. (A) Cy3-modified DNA duplex oligomers. (B) Cy5-modified DNA duplex oligomers.

Table 3
Parameters of the next-nearest-neighbor model (NNN) for stabilizing effects of Cy3 and Cy5 dyes attached to 5′ terminus of DNA·DNA duplexes.

Sequence[a]	$\Delta\Delta H^\circ$ (kcal.mol^{-1})	$\Delta\Delta S^\circ$ (cal.mol^{-1}.K^{-1})	$\Delta\Delta G^\circ_{37}$ (kcal.mol^{-1})
Cy3–AA/TT	−3.20	−7.37	−0.91
Cy3–AC/TG	−3.81	−8.20	−1.27
Cy3–AG/TC	−3.26	−7.23	−1.02
Cy3–AT/TA	−5.79	−14.70	−1.23
Cy3–CA/GT	−4.99	−11.63	−1.39
Cy3–CC/GG	−2.24	−3.01	−1.30
Cy3–CG/GC	−4.27	−8.85	−1.53
Cy3–CT/GA	−1.99	−2.16	−1.32
Cy3–GA/CT	−2.99	−5.59	−1.26
Cy3–GC/CG	−2.28	−3.61	−1.16
Cy3–GG/CC	−6.37	−15.96	−1.42
Cy3–GT/CA	−2.97	−6.03	−1.10
Cy3–TA/AT	−2.08	−3.92	−0.87
Cy3–TC/AG	−1.09	0.08	−1.12
Cy3–TG/AC	−4.96	−11.82	−1.29
Cy3–TT/AA	−3.67	−8.32	−1.09
Cy5–AA/TT	0.62	3.78	−0.55
Cy5–AC/TG	−3.16	−6.24	−1.22
Cy5-AG/TC	−2.57	−5.11	−0.99
Cy5–AT/TA	−3.01	−6.41	−1.02
Cy5–CA/GT	−3.76	−7.72	−1.36
Cy5–CC/GG	0.33	5.06	−1.24
Cy5–CG/GC	−4.25	−8.95	−1.47
Cy5–CT/GA	−1.71	−0.96	−1.41
Cy5–GA/CT	−1.55	−1.50	−1.09
Cy5–GC/CG	1.11	5.73	−0.67
Cy5–GG/CC	−1.19	−0.78	−0.95
Cy5–GT/CA	−2.47	−4.45	−1.09
Cy5–TA/AT	−3.49	−7.74	−1.09
Cy5–TC/AG	−3.60	−6.66	−1.54
Cy5–TG/AC	−3.49	−7.11	−1.29
Cy5–TT/AA	−8.29	−21.93	−1.48

[a] Sequence orientation is 5′–DNA–3′/3′–DNA–5′.

attributed to dyes. The results are revealed in Table 4. The left side of the table shows performance of predictions for the primary data set that was also used to derive the parameters. The next-nearest-neighbor model exhibits the lowest χ^2 and the lowest rmsd values for predictions of both Gibbs energy contributions and ΔT_m values. It is not surprising that the more complex NNN model fits the primary dataset better than the 1P or NN models. Increasing the number of parameters usually improves fit to a data set. The better measure of accuracy is the model ability to predict set of independent measurements that were not used to determine model parameters.

We have measured validation melting data for both Cy3 and Cy5 modified oligonucleotides. The sequences ranged in length from 10 to 30 base pairs and GC base pair content varied from 30 to 60%. Melting temperatures of independent validation set are reported in Table 5. Ability of thermodynamic models to predict ΔT_m values of the validation set is analyzed in the last two columns of Table 4. Again, the next-nearest-neighbor model exhibits the best accuracy, the lowest χ^2 and the lowest rmsd, compared to the 1P and NN models. We therefore recommend using the NNN model and the parameters from Table 3 to make stability predictions for Cy3- and Cy5-modified duplexes.

3.4 . Interactions between Cy dyes and dangling nucleotides

In many biological experiments, the complementary strand is longer than the oligonucleotide probe labeled with a dye. The questions arise about energetics of interactions between dangling (unpaired) nucleotides of the complementary strand and the attached dye. We have studied several modifications of the core oligonucleotide duplex D6 where the complementary strand was extended at 3′ end with various native nucleotides. The Gibbs energy of hybridization for these duplexes was compared with the core duplex and with the Cy3-modified duplexes. Analysis of experimental data is presented in Table 6. The $\Delta\Delta G^\circ$ values are calculated using the core duplex as a reference. The 3rd column of the table contains measured Gibbs energy of stabilization due to the dangling ends. The 4th column shows the measured $\Delta\Delta G^\circ$ contribution from the attached Cy3 dye. The sum of these two contributions is calculated in the 5th column. The last, 6th column shows experimentally measured Gibbs contribution when both the dangling nucleotide and the Cy3 dye were attached to the duplex. The values in the 5th column and the last column are identical within experimental errors. This comparison demonstrates that the effects of dangling nucleotides and the Cy3 dye are approximately additive. We have repeated the study for a different sequence, duplex ID D5. The results are shown in the bottom of Table 6. Again, the $\Delta\Delta G^\circ_{37}$ contributions are additive. The additivity of Cy3 and dangling end effects seems to hold for various sequences.

4 . Discussion

Chemical synthesis of cyanine modified oligonucleotides is challenging and expensive. It would be therefore useful to predict accurately hybridization of these oligonucleotides and design them well for applications and experiments. In addition, knowledge of dye–DNA interactions is important for development of new modifications and interpretations of fluorescence measurements. Current algorithms assume that the attached dyes do not change significantly thermodynamic stability of DNA duplexes and the effects of terminal labels are often neglected. Our experiments demonstrate that this approach gives inaccurate predictions of melting temperatures and transition Gibbs energies. For short oligomers (less than 15 base pairs), T_m increased up to 7.6 °C per attached Cy dye (Table 1). The increase is significant even for long oligomers. Table 5 shows stabilization up to 2.6 °C for 20 base pair long duplexes. This is consistent with our previous study detecting ~1.5 °C increase of T_m when 20-mer duplex is modified with either Cy5 or Cy3 [29]. Similar values have been observed by others [22]. Character

Table 4
Accuracy of predictions for hybridization thermodynamics of Cy3- and Cy5-modified DNA duplexes.

Model[a]	No. param.	Predictions for primary set		Predictions for validation set		
		$\chi^2(\Delta\Delta G)$	$\chi^2(\Delta T_m)$	rmsd(ΔT_m)[b]	$\chi^2(\Delta T_m)$	rmsd(ΔT_m)[b]
Cy3 dye attached to 5' terminus						
1P	1	18	21	0.7	8.1	0.5
NN	4	11	16	0.6	7.7	0.5
NNN	10	1.2	8.3	0.5	3.4	0.3
Cy5 dye attached to 5' terminus						
1P	1	40	42	1.1	11.8	0.6
NN	4	17	17	0.7	13.1	0.6
NNN	10	(0)	7.1	0.5	9.7	0.5

[a] Parameters of models NNN, 1P, and NN are in Table 3 and S2.
[b] Units are °C.

of the linker influences the magnitude of duplex stabilization. The rigid linker, *e.g.* triple C≡C bond, restricts the cyanine dye mobility and appears to prevent interactions between the dye and the DNA duplex. In this case, the attachment of Cy3 or Cy5 dye does not change duplex stability [22]. If the aliphatic linker made from CH_2–CH_2 bonds is used, the flexible chain allows the dye to interact with neighbor nucleotides and explore various conformations. Fegan et al. reported that the flexible attachment of Cy dyes to the terminal dT base stabilized 15 base pair duplex by 8 to 9 °C [22].

In contrast, the Cy3 and Cy5 dyes attached in the *interior* of the duplex are usually destabilizing [2,23,40]. The magnitude of this effect is also dependent on the character of the linker. The dye attached by a single alkane linker to a nucleobase appears to reduce T_m more than the dye inserted between nucleotides as a part of the DNA backbone [2]. The flexible linker *alone* does not appear to be responsible for the change of duplex stability; the presence of the dye is required to observe the destabilization [23]. All these results show that it is necessary to account for the dye and the linker contributions to duplex stability to make accurate predictions. The stabilizing effects have the most impact in short duplexes that are seen in hairpins, molecular beacons, and nanostructures.

The analysis in Fig. 3 and the parameters in Table 3 demonstrate that the thermodynamic effects of Cy3 and Cy5 depend on the base sequence. This has been seen also for fluorescence properties of the dyes. Fluorescence lifetimes, anisotropy and quantum yields depend on the local environment and the base sequence near the site of attachment [24,41]. This sensitivity has been explained in terms of cis-trans isomerization of C=C bonds in the dye polymethine chain [24]. The bonds are primarily in the all-trans conformation in the ground state. Upon excitation, isomerization competes with fluorescence emission for deactivation of the molecule from the excited to the ground state. If the photoisomerization is sterically obstructed by dye–DNA interactions, fluorescence efficiency and lifetime increases.

Interactions between small organic molecules and nucleic acids have been characterized based on structural attributes. The Cy dyes have the geminal methyl groups that has been suggested to suppress intercalation and groove binding due to steric clashes [42]. These two modes of dye–DNA interactions are usually accompanied by substantial changes of absorbance spectrum, specifically, peak shapes, magnitudes, and maximum wavelengths change [43]. We have not detected any such spectral changes when the complementary strand hybridized to Cy3- or Cy5-modified oligonucleotides (data not shown).

NMR structural experiments established that both Cy3 and Cy5 dyes are mostly stack onto the terminal base pair, in a similar orientation to an additional base pair [44,45]. This notion is in agreement with observed periodicity of FRET efficiency [20]. However, the rise of Cy3 ring is larger than the rise between bases in B-DNA duplex (0.5 nm vs 0.34 nm). The proximal indole ring, to which DNA linker is attached, partially stacks and exhibits weak interactions with the neighbor base. The distal indole ring makes strong interactions with the base *complementary* to the nucleotide of the dye attachment. We hypothesize that this interaction is crucial for the sequence specificity of duplex stabilization. If Cy dye is attached to pyrimidine, it exhibit strong stacking interactions with the complementary purine. Therefore, the stabilizing free energy contributions are generally large (Fig. 3). If the dye is conjugated to purine nucleotide, it stacks and interacts less with the complementary pyrimidine. Gibbs energy contribution to duplex stability is therefore smaller than in the first case. We assume that dye–nucleobase π–π

Table 5
Validation set of modified duplexes that were not used to derive thermodynamic parameters.

Sequence (5′ to 3′)[a]	Exper. T_m (°C)		ΔT_m (°C)	
	Modified duplex	Core DNA	Exper.[b]	Predict.[c]
Cy3–GAAATGAAAG	39.1	33.6	5.5	5.4
Cy3–CGTACACATGC	54.4	49.5	4.9	5.2
Cy3–TGATTCTACCTATGTGATTT	65.4	63.4	2.0	2.2
Cy3–TGAGGTAGACACAATGATGG	70.5	68.6	1.9	2.0
Cy3–ACCGACGACGCTGATCCGAT	80.4	77.8	2.6	2.0
Cy3–GTTCACGTCCGAAAGCTCGAAAAAGGATAC	79.6	78.7	0.9	1.2
Cy5–GAAATGAAAG	38.4	33.6	4.8	4.7
Cy5–CGTACACATGC	54.0	49.5	4.5	5.0
Cy5–TGATTCTACCTATGTGATTT	66.0	63.4	2.6	2.5
Cy5–TGAGGTAGACACAATGATGG	69.8	68.6	1.2	2.4
Cy5–ACCGACGACGCTGATCCGAT	79.4	77.8	1.6	2.1
Cy5–GTTCACGTCCGAAAGCTCGAAAAAGGATAC	80.1	78.7	1.4	1.3

[a] Complementary sequence is the perfectly matched DNA oligomer that is not chemically modified.
[b] Experimentally measured T_m difference between modified and core DNA duplexes (C_t = 2 μM, 1 M Na^+ buffer).
[c] Predicted T_m difference using NNN thermodynamic parameters from Table 3 and unified parameters [26].

Table 6
Experimentally measured thermodynamic contributions of Cy3 dyes and dangling nucleotides.

DNA duplex	Dangling base (X)	Attached base $\Delta\Delta G^\circ$(X)[a] (kcal·mol^{-1})	Attached Cy3 $\Delta\Delta G^\circ$(Cy3)[b] (kcal·mol^{-1})	Sum of $\Delta\Delta G^\circ$(X) and $\Delta\Delta G^\circ$(Cy3) (kcal·mol^{-1})	Attached both X and Cy3 $\Delta\Delta G^\circ$(both) (kcal·mol^{-1})
Cy3-CCGATGCC/ X-GGCTACGG	A	−0.4	−1.3	−1.7	−1.8
	C	+0.2	−1.3	−1.1	−1.4
	G	−0.4	−1.3	−1.7	−1.6
	T	−0.3	−1.3	−1.6	−1.7
Cy3-AGCGTCCA/ X-TCGCAGGT	A	−0.4	−1.2	−1.6	−1.6
	C	−0.2	−1.2	−1.4	−1.6
	G	−0.4	−1.2	−1.6	−1.6
	T	−0.4	−1.2	−1.6	−1.6

[a] Only dangling base was attached to duplex terminus (no Cy3 dye). $\Delta\Delta G^\circ(X) = \Delta G^\circ_{37}$(duplex with dangling base) − ΔG°_{37}(core duplex). Transition Gibbs energies were determined from fits to melting profiles. Experiments were conducted in a 1 M Na^+ buffer and C_t was 5 μM.
[b] Only Cy3 was attached to duplex terminus (no dangling base).

stacking interactions are stronger for purines than pyrimidines due to the size of nucleobase conjugated ring system. Harvey and Levitus measured interactions between Cy3 dyes and deoxyribonucleoside monophosphates (dNMP) in solution [46]. Purine dNMP enhanced Cy3 fluorescence quantum yield and lifetimes substantially more than pyridine dNMPs. Their fluorescence results established that Cy3-nucleotide interactions are stronger for purine than pyrimidine nucleotides in agreement with our hypothesis of duplex stabilization specificity.

The measurements of Iqbal et al. demonstrate that the stacking interactions of the dyes are dynamic [20]. FRET efficiency between Cy3 and Cy5 deviates from the rigid structure predictions suggesting that lateral movements and alternative stacked conformations may occur. Multiple fluorescent lifetimes also indicate that a minor fraction of dyes is unstacked and free to explore various conformations [21]. In spite of the alternative conformations, thermodynamic data fits the assumption of two-state melting process. The dominant conformation of attached Cy3 and Cy5 dyes is being stack on the terminal base pair. The dyes stabilize duplexes and suppress fraying of duplex termini.

Recently, Kroutil et al. published computer modeling of Cy3 and Cy5 dyes attached to 5′ end of CCACTAGTGG sequence [51]. They reported significant stacking between the distal indole ring of dyes and the complementary guanine. This stacking interaction was detected in the most probable structures. The stacked dye also changed the local flexibility reaching up to two neighbor base pairs. The largest structural impact was detected at the first, nearest neighbor base pair. These findings are consistent with our sequence dependence of measured Gibbs energies and with the necessity to consider two neighbor base pairs in the thermodynamic model.

Average Gibbs energy contributions are similar for both Cy3 and Cy5 because the dyes have analogous chemical structures and interactions with DNA. The Cy5 dye contains two extra methine groups in the chain that is bridging indole rings. The long bridge seems to decrease interactions of the proximal indole ring with DNA [44], which may explain minor differences between dyes. Table 3 shows that the duplex stabilization is enthalpically driven for the vast majority of sequences. The exceptions are three Cy5 parameters, Cy5–AA/TT, Cy5–CC/GG, and Cy5–GC/CG, where the stabilization is characterized by favorable decrease of entropic cost for duplex formation. The contributions of various forces (electrostatic, dispersion, hydrophobic, and van der Waals) are likely to be specific for each dye and sequence context [47].

It is important to consider limitations of the new thermodynamic model. The parameters were determined for 5′ attachments of the dyes with the standard three-carbon flexible linker. If the linker has different length or is rigid, the thermodynamic contributions of the dyes could be different [22,48]. In addition, the point of the dye conjugation matters. Molecular dynamics simulations suggest that 3′ attached dyes explore a wide region of configuration space and stacking interactions are weak compared to 5′ attached dyes [49]. The Cy dyes conjugated to duplex interior are destabilizing [2]; new parameters are not applicable in this case.

New parameters have been determined for duplexes folded into B-DNA structure; the other secondary structures may exhibit different interactions. For example, free Cy5 has been found to stabilize the telomeric quadruplex more than the duplex [50]. Another factor that could affect dye interactions is the presence of other modifications in the close proximity. If a quencher is attached at the same duplex end, the dye–quencher complex is likely to form. These complexes stabilize duplexes significantly more than any Cy dye alone [39]. Finally, the thermodynamic parameters were determined at neutral pH and in 1 M Na^+ buffer. The values may be different in buffers deviating from these conditions.

5 . Conclusions

We have determined thermodynamic parameters to improve prediction of DNA duplex stability where Cy3 or Cy5 dye is attached to oligonucleotide 5′ terminus. The stabilizing effects of dyes are sequence-dependent and larger than the thermodynamic effects of dangling nucleotides. New parameters will be implemented into free on-line calculation tool at http://biophysics.idtdna.com.

Acknowledgments

We thank to Shawn Eyestone and Erica Lautner for performing measurements of mass spectra. We would also like to thank David Lilley and David Norman for providing the coordinates of their NMR structure of the Cy3-oligonucleotide. This work was funded by Integrated DNA Technologies, Inc.

Appendix A. Supplementary data

Example of T_m, ΔG° predictions, table of duplex concentrations in melting experiments and figures showing $1/T_m$ vs ln C_t fits. Supplementary data associated with this article can be found in the online version, at http://dx.doi.org/10.1016/j.bpc.2015.01.001.

References

[1] S. Weiss, Fluorescence spectroscopy of single biomolecules, Science 283 (1999) 1676–1683.
[2] W. Lee, P.H. von Hippel, A.H. Marcus, Internally labeled Cy3/Cy5 DNA constructs show greatly enhanced photo-stability in single-molecule FRET experiments, Nucleic Acids Res. 42 (2014) 5967–5977.
[3] P.S. Bernard, M.J. Lay, C.T. Wittwer, Integrated amplification and detection of the C677T point mutation in the methylenetetrahydrofolate reductase gene by fluorescence resonance energy transfer and probe melting curves, Anal. Biochem. 255 (1998) 101–107.
[4] V.V. Didenko, DNA probes using fluorescence resonance energy transfer (FRET): designs and applications, Biotechniques 31 (2001) 1106–1121.

[5] G. Bonnet, S. Tyagi, A. Libchaber, F.R. Kramer, Thermodynamic basis of the enhanced specificity of structured DNA probes, Proc. Natl. Acad. Sci. U. S. A. 96 (1999) 6171–6176.
[6] C.A. Heid, J. Stevens, K.J. Livak, P.M. Williams, Real time quantitative PCR, Genome Res. 6 (1996) 986–994.
[7] C.T. Wittwer, M.G. Herrmann, C.N. Gundry, K.S.J. Elenitoba-Johnson, Real-time multiplex PCR assays, Methods 25 (2001) 430–442.
[8] X. Zhou, J. Zhou, Improving the signal sensitivity and photostability of DNA hybridizations on microarrays by using dye-doped core–shell silica nanoparticles, Anal. Chem. 76 (2004) 5302–5312.
[9] M. Schena, D. Shalon, R. Heller, A. Chai, P.O. Brown, R.W. Davis, Parallel human genome analysis: microarray-based expression monitoring of 1000 genes, Proc. Natl. Acad. Sci. U. S. A. 93 (1996) 10614–10619.
[10] A. Tsourkas, M.A. Behlke, S.D. Rose, G. Bao, Hybridization kinetics and thermodynamics of molecular beacons, Nucleic Acids Res. 31 (2003) 1319–1330.
[11] A.P. Silverman, E.T. Kool, Oligonucleotide probes for RNA-targeted fluorescence in situ hybridization, Adv. Clin. Chem. 43 (2007) 79–115.
[12] C. Albrecht, K. Blank, M. Lalic-Mülthaler, S. Hirler, T. Mai, I. Gilbert, S. Schiffmann, T. Bayer, H. Clausen-Schaumann, H.E. Gaub, DNA: a programmable force sensor, Science 301 (2003) 367–370.
[13] N. Di Fiori, A. Meller, The effect of dye–dye interactions on the spatial resolution of single-molecule FRET measurements in nucleic acids, Biophys. J. 98 (2010) 2265–2272.
[14] J. Malicka, I. Gryczynski, J. Fang, J.R. Lakowicz, Fluorescence spectral properties of cyanine dye-labeled DNA oligomers on surfaces coated with silver particles, Anal. Biochem. 317 (2003) 136–146.
[15] M. Heilemann, E. Margeat, R. Kasper, M. Sauer, P. Tinnefeld, Carbocyanine dyes as efficient reversible single-molecule optical switch, J. Am. Chem. Soc. 127 (2005) 3801–3806.
[16] A.L. Lucius, C. Jason Wong, T.M. Lohman, Fluorescence stopped-flow studies of single turnover kinetics of *E. coli* RecBCD helicase-catalyzed DNA unwinding, J. Mol. Biol. 339 (2004) 731–750.
[17] M. Mihalusova, J.Y. Wu, X. Zhuang, Functional importance of telomerase pseudoknot revealed by single-molecule analysis, Proc. Natl. Acad. Sci. U. S. A. 108 (2011) 20339–20344.
[18] S.A.E. Marras, F.R. Kramer, S. Tyagi, Efficiencies of fluorescence resonance energy transfer and contact-mediated quenching in oligonucleotide probes, Nucleic Acids Res. 30 (2002) e122.
[19] S. Sindbert, S. Kalinin, H. Nguyen, A. Kienzler, L. Clima, W. Bannwarth, B. Appel, S. Müller, C.A.M. Seidel, Accurate distance determination of nucleic acids via Förster resonance energy transfer: implications of dye linker length and rigidity, J. Am. Chem. Soc. 133 (2011) 2463–2480.
[20] A. Iqbal, S. Arslan, B. Okumus, T.J. Wilson, G. Giraud, D.G. Norman, T. Ha, D.M.J. Lilley, Orientation dependence in fluorescent energy transfer between Cy3 and Cy5 terminally attached to double-stranded nucleic acids, Proc. Natl. Acad. Sci. U. S. A. 105 (2008) 11176–11181.
[21] M.E. Sanborn, B.K. Connolly, K. Gurunathan, M. Levitus, Fluorescence properties and photophysics of the sulfoindocyanine Cy3 linked covalently to DNA, J. Phys. Chem. B 111 (2007) 11064–11074.
[22] A. Fegan, P.S. Shirude, S. Balasubramanian, Rigid cyanine dye nucleic acid labels, Chem. Commun. (2008) 2004–2006.
[23] J.B. Randolph, A.S. Waggoner, Stability, specificity and fluorescence brightness of multiply-labeled fluorescent DNA probes, Nucleic Acids Res. 25 (1997) 2923–2929.
[24] M. Levitus, S. Ranjit, Cyanine dyes in biophysical research: the photophysics of polymethine fluorescent dyes in biomolecular environments, Q. Rev. Biophys. 44 (2011) 123–151.
[25] R. Owczarzy, P.M. Vallone, F.J. Gallo, T.M. Paner, M.J. Lane, A.S. Benight, Predicting sequence-dependent melting stability of short duplex DNA oligomers, Biopolymers 44 (1997) 217–239.
[26] J. SantaLucia Jr., A unified view of polymer, dumbbell, and oligonucleotide DNA nearest-neighbor thermodynamics, Proc. Natl. Acad. Sci. U. S. A. 95 (1998) 1460–1465.
[27] T. Xia, J. SantaLucia Jr., M.E. Burkard, R. Kierzek, S.J. Schroeder, X. Jiao, C. Cox, D.H. Turner, Thermodynamic parameters for an expanded nearest-neighbor model for formation of RNA duplexes with Watson–Crick base pairs, Biochemistry 37 (1998) 14719–14735.
[28] A.R. Davis, B.M. Znosko, Thermodynamic characterization of single mismatches found in naturally occurring RNA, Biochemistry 46 (2007) 13425–13436.
[29] B.G. Moreira, Y. You, M.A. Behlke, R. Owczarzy, Effects of fluorescent dyes, quenchers, and dangling ends on DNA duplex stability, Biochem. Biophys. Res. Commun. 327 (2005) 473–484.
[30] R. Owczarzy, Y. You, B.G. Moreira, J.A. Manthey, L. Huang, M.A. Behlke, J.A. Walder, Effects of sodium ions on DNA duplex oligomers: improved predictions of melting temperatures, Biochemistry 43 (2004) 3537–3554.
[31] G.D. Fasman, Handbook of Biochemistry and Molecular Biology, CRC Press, Cleveland, OH, 1975.
[32] R. Owczarzy, Melting temperatures of nucleic acids: discrepancies in analysis, Biophys. Chem. 117 (2005) 207–215.
[33] L.A. Marky, K.J. Breslauer, Calculating thermodynamic data for transitions of any molecularity from equilibrium melting curves, Biopolymers 26 (1987) 1601–1620.
[34] P.N. Borer, B. Dengler, I. Tinoco Jr., O.C. Uhlenbeck, Stability of ribonucleic acid double-stranded helices, J. Mol. Biol. 86 (1974) 843–853.
[35] M. Petersheim, D.H. Turner, Base-stacking and base-pairing contributions to helix stability: thermodynamics of double-helix formation with CCGG, CCGGp, CCGGAp, ACCGGp, CCGGUp, and ACCGGUp, Biochemistry 22 (1983) 256–263.
[36] J. Applequist, V. Damle, Thermodynamics of the helix-coil equilibrium in oligoadenylic acid from hypochromicity studies, J. Am. Chem. Soc. 87 (1965) 1450–1458.
[37] R. Owczarzy, Y. You, C.L. Groth, A.V. Tataurov, Stability and mismatch discrimination of locked nucleic acid–DNA duplexes, Biochemistry 50 (2011) 9352–9367.
[38] S.J. Schroeder, D.H. Turner, Optical melting measurements of nucleic acid thermodynamics, Methods Enzymol. 468 (2009) 371–387.
[39] Y. You, A.V. Tataurov, R. Owczarzy, Measuring thermodynamic details of DNA hybridization using fluorescence, Biopolymers 95 (2011) 472–486.
[40] L.M. Hall, M. Gerowska, T. Brown, A highly fluorescent DNA toolkit: synthesis and properties of oligonucleotides containing new Cy3, Cy5 and Cy3B monomers, Nucleic Acids Res. 40 (2012) e108.
[41] B.J. Harvey, C. Perez, M. Levitus, DNA sequence-dependent enhancement of Cy3 fluorescence, Photochem. Photobiol. Sci. 8 (2009) 1105–1110.
[42] B.A. Armitage, Cyanine dye–DNA interactions: intercalation, groove binding, and aggregation, Top. Curr. Chem. 253 (2005) 55–76.
[43] K.C. Hannah, R.R. Gil, B.A. Armitage, 1H NMR and optical spectroscopic investigation of the sequence-dependent dimerization of a symmetrical cyanine dye in the DNA minor groove, Biochemistry 44 (2005) 15924–15929.
[44] A. Iqbal, L. Wang, K.C. Thompson, D.M.J. Lilley, D.G. Norman, The structure of cyanine 5 terminally attached to double-stranded DNA: implications for FRET studies, Biochemistry 47 (2008) 7857–7862.
[45] D.G. Norman, R.J. Grainger, D. Uhrin, D.M.J. Lilley, Location of cyanine-3 on double-stranded DNA: importance for fluorescence resonance energy transfer studies, Biochemistry 39 (2000) 6317–6324.
[46] B.J. Harvey, M. Levitus, Nucleobase-specific enhancement of Cy3 fluorescence, J. Fluoresc. 19 (2009) 443–448.
[47] K.M. Guckian, B.A. Schweitzer, R.X.F. Ren, C.J. Sheils, D.C. Tahmassebi, E.T. Kool, Factors contributing to aromatic stacking in water: evaluation in the context of DNA, J. Am. Chem. Soc. 122 (2000) 2213–2222.
[48] J. Ouellet, S. Schorr, A. Iqbal, T.J. Wilson, D.M.J. Lilley, Orientation of cyanine fluorophores terminally attached to DNA via long, flexible tethers, Biophys. J. 101 (2011) 1148–1154.
[49] P. Milas, B.D. Gamari, L. Parrot, B.P. Krueger, S. Rahmanseresht, J. Moore, L.S. Goldner, Indocyanine dyes approach free rotation at the 3′ terminus of A-RNA: a comparison with the 5′ terminus and consequences for fluorescence resonance energy transfer, J. Phys. Chem. B 117 (2013) 8649–8658.
[50] R. Nanjunda, E.A. Owens, L. Mickelson, S. Alyabyev, N. Kilpatrick, S. Wang, M. Henary, W.D. Wilson, Halogenated pentamethine cyanine dyes exhibiting high fidelity for G-quadruplex DNA, Bioorg. Med. Chem. 20 (2012) 7002–7011.
[51] O. Kroutil, I. Romancová, M. Šíp, Z. Chval, Cy3 and Cy5 dyes terminally attached to 5′ C end of DNA: structure, dynamics, and energetics, J. Phys. Chem. B 118 (2014) 13564–13572.